Research Article

Stabilization of chaotic systems via act-and-wait delayed feedback control using a high-precision direct integration method

Dasheng Liu[1,2] · Guozheng Yan[2]

Received: 14 November 2019 / Accepted: 19 February 2020 / Published online: 2 March 2020

Abstract
A technique for the numerical analysis of the stability problem in chaotic systems via act-and-wait delayed feedback control is developed and justified. Recently, act-and-wait modification of a delayed feedback control method is proposed to stabilize unstable periodic orbits in dynamical systems. To overcome the difficulties in obtaining conditions under which the state of closed-loop system converges toward a periodic solution via the act-and-wait scheme, this paper presents a high-precision direct integration method for calculating the monodromy matrix corresponding to the closed-loop system based on the theory of Peano–Baker series. The capabilities of the proposed schemes in stabilization of unstable periodic orbits of chaotic systems are illustrated by numerical examples.

Keywords Chaos control · Delayed feedback control · Direct integration method · Act-and-wait · Monodromy matrix

1 Introduction

Scientists have found that unexpected evolution patterns arise frequently in numerous nonlinear systems in physics, chemistry, biology, engineering, economics, and so forth. The most peculiar aspect of these patterns is their random-like behavior although the systems are deterministic, ie., the deterministic nature of these systems does not make them predictable. This behavior is known as chaos which is due to sensitive dependence on the initial conditions. It has been known that chaotic dynamics [1–10] generally consists of a motion where the nonlinear system state moves for a while in the neighborhood of one of the unstable periodic orbits(UPOs) and then falls close to a different unstable periodic orbit. Based on this fact, Ott et al. [11] proposed the first strategy to stabilize UPOs utilizing the sensitivity to initial conditions. From then on, chaos control has received a great deal of interests among the researchers, and a variety of chaotic systems have been proven to be able to be stabilized by several different techniques such as delayed feedback control(DFC) [12–19], prediction-based control [20–22], robust control [23, 24], slide mode control [25–27], adaptive control [28–30], energy-based feedback control [31].

Among them, delayed feedback control [12] has gained wide acceptance due to that the control input vanishes after the stabilization is achieved. Although the DFC is successful in various chaotic systems, the stability analysis of the closed-loop system often does not have an analytical form. One of the reasons is that the dynamics is described by a delay differential equation(DDE). Furthermore, some researchers have given several analytical results [32, 33], showing that the DFC has an odd number limitation. Since then, several improved DFC methods including extended DFC [8, 34–38], periodic DFC [39–42], and double delayed feedback control (DDFC) [43] have been developed to make the DFC more applicable. Recently, the DFC has been extended to solve practical application problems in

✉ Dasheng Liu, dsliu@sjtu.edu.cn | [1]Department of Instrument Science and Engineering, School of Electronic Information and Electrical Engineering, Shanghai Jiao Tong University, Shanghai 200240, China. [2]National Center for Translational Medicine, Collaborative Innovational Center for System Biology, Shanghai Jiao Tong University, Shanghai 200240, China.

engineering. For example, Wu et al. [44] investigated the effects of a delayed feedback scheme in the parameter space and demonstrated that wave segments can be stabilized. Costa and Savi [45] applied the extended DFC on a smart system composed of a pendulum coupled with shape-memory alloy elements. Paul and Banerjee [46] proposed a nonlocal time-delayed feedback control technique to control the spatiotemporal patterns in coupled map lattice(CML) systems and demonstrated its efficacy in a network of coupled digital phase-locked loops which is real-world CML system.

Although the delay differential equations usually have infinite-dimensional phase spaces, its stability can be described by an infinite-dimensional transition matrix [47]. The system is considered to be asymptotically stable if all the characteristic multipliers of the corresponding transition matrix are in modulus less than one. Insperger [48] proposed an act-and-wait control concept for continuous-time systems with feedback delay associated with infinite poles. The control strategy is that the feedback input is periodically switched on and off. It has been shown that if the waiting duration is larger than the feedback delay time, then the system is represented by a finite-dimensional monodromy matrix and the stability can be described by a finite number of eigenvalues. Thus, the infinite-dimensional pole placement problem is reduced to a finite-dimensional one.

The act-and-wait control method is an effective technique to reduce the number of poles for systems with large feedback delay, which makes the pole placement problem easier. In recent years, act-and-wait concept has been further tested through experiments [49] and theoretically extended to discrete-time systems [50], autonomous systems [51], non-autonomous dynamical systems [52], linear periodic time-varying systems [53, 54], etc. [55–58]. Act-and-wait scheme requires to obtain the monodromy matrix associated with the closed-loop system. However, it is usually hard to find a homogeneous expression of the corresponding monodromy matrix, due to the existence of the delay term. Based on a high-precision direct integration algorithm [59, 60], this paper explores the stabilization of periodic solutions to chaotic systems with an act-and-wait-fashioned delayed feedback control framework.

The paper aims to overcome the difficulties in obtaining stability conditions of the chaotic systems under the act-and-wait DFC and presents a high-precision direct integration method for calculating the monodromy matrix corresponding to the closed-loop system. The rest of the paper is organized as follows: Sect. 2 introduces the act-and-wait modification of DFC and formulates the condition where the controlled system becomes to be finite dimensional. Section 3 discusses the linear stability analysis of UPOs controlled by act-and-wait delayed feedback control and presents a periodically time-varying precise integration method for calculating the monodromy matrix corresponding to the closed-loop system. In Sec. 4, it is given two illustrative numerical examples to show the effectiveness of the proposed method. Finally, it is concluded in Sect. 5.

2 Problem formulation

Consider an nth-order nonlinear system which shows a chaotic behavior described by an n-dimensional first-order vector differential equation as follows:

$$\dot{\mathbf{x}}(t) = f(\mathbf{x}(t), u(t)), \tag{1}$$

where $\mathbf{x} \in \mathfrak{R}^n$ is the state vector, $\dot{\mathbf{x}}$ denotes the derivative of $\mathbf{x}$ with respect to the time variable t, $u \in \mathfrak{R}^m$ is the control input, $f(\cdot)$ is an n-dimensional nonlinear vector function and assumed to be continuously differentiable. Suppose that the uncontrolled system has a T-periodic solution $\mathbf{x}(t) = \xi(t) = \xi(t+T)$ that satisfies the equation $\dot{\xi}(t) = f(\xi(t), 0)$ and in a chaotic state. The task is to design a control law to suppress the chaotic behavior and make a more regular motion which may be a periodic motion. Many nonlinear dynamical systems in engineering science can be described by the above general set of differential equation, such as pendulum, mass-spring mechanical system, oscillator, microbeams. [1, 40, 61, 62].

The delayed feedback control (DFC) [34] is given by

$$u(t) = K(\mathbf{x}(t) - \mathbf{x}(t-T)), \tag{2}$$

where K is the gain matrix of the controller. In the delayed feedback control method, since the control input $u(t)$ is computed based on the difference between the current state and the delayed state, $u(t)$ vanishes after the UPO is stabilized. Although DFC can be relatively simply implemented in experiments, its theory is rather difficult, since the time-delay dynamics takes place in infinite-dimensional phase spaces. Generally, it is difficult to determine the feedback gain with which the desired UPO is stabilized.

As shown in Fig. 1, the act-and-wait controller is introduced as follows:

$$u(t) = s(t)K(\mathbf{x}(t) - \mathbf{x}(t-T)), \tag{3}$$

where $s(t)$ is a T-periodic function that switches the controller on and off alternately at every integer multiples of the period T defined as

$$s(t) = \begin{cases} 0 & \text{if } 0 \le (t \bmod 2T) < T, \\ 1 & \text{if } T \le (t \bmod 2T) < 2T. \end{cases} \tag{4}$$

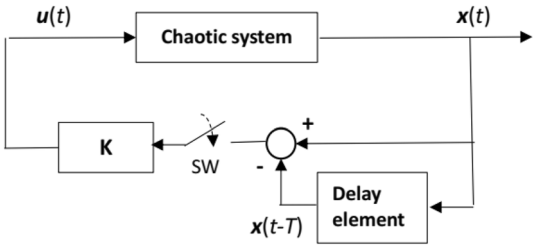

Fig. 1 Block diagram of a chaotic system under the act-and-wait DFC

The act-and-wait control method is originally used for *n*-dimensional continuous-time control systems with feedback delay. It has been shown that the infinite-dimensional pole placement problem of the delayed system can be reduced to an *n*-dimensional one, if the feedback is periodically switched off and on. The point is that the switched system can be described by a monodromy matrix, consequently, stability properties are described by *n* eigenvalues.

3 Stability analysis of act-and-wait DFC

The closed-loop system is linearized around the UPO,$\xi(t)$:

$$\begin{cases} \delta\dot{\mathbf{x}}(t) = A(t)\delta\mathbf{x}(t) + B(t)u(t), \\ u(t) = s(t)K(\delta\mathbf{x}(t) - \delta\mathbf{x}(t-T)), \end{cases} \tag{5}$$

where $\delta\mathbf{x}(t) := \mathbf{x}(t) - \xi(t)$ is the deviation of the solution from the target UPO, and $\delta\mathbf{x}(t-T)$ is its T-delayed version. The T-periodic matrixes $A(t)$, $B(t)$ are the Jacobian matrixes of the system evaluated on the UPO such that,

$$\begin{aligned} A(t) &\triangleq \frac{\partial f(\mathbf{x}(t), u(t))}{\partial \mathbf{x}}|_{\mathbf{x}=\xi(t),u(t)=0}, \\ B(t) &\triangleq \frac{\partial f(\mathbf{x}(t), u(t))}{\partial u}|_{\mathbf{x}=\xi(t),u(t)=0}. \end{aligned} \tag{6}$$

Here, note that the linearized version of the closed-loop system (5) is locally asymptotically stable at the UPO. Moveover, system (5) is similar to a linear periodic time-varying system such that [54]

$$\dot{x}(t) = (A(t) + B(t)s(t)K)x(t) - B(t)s(t)Kx(t-T), \tag{7}$$

where $x(t) \in \mathfrak{R}^n$ is the state vector. From Eqs. (7) and (4), if $t \in [2kT, 2kT+T), k = 0, 1, 2, \ldots$, then

$$\dot{x}(t) = A(t)x(t), \tag{8}$$

while if $t \in [2kT+T, 2kT+2T), k = 0, 1, 2, \ldots$, then

$$\dot{x}(t) = (A(t) + B(t)K)x(t) - B(t)Kx(t-T). \tag{9}$$

3.1 Monodromy matrix of the closed-loop system

If we define the state-transition matrix of system (8) to be $M(\cdot)$, the monodromy matrix associated with the T-periodic system can be given by $M(T,0) \in \mathfrak{R}^{n\times n}$. Moreover, define $\Gamma(\cdot)$ as the state-transition matrix for the periodic system

$$\dot{x}(t) = (A(t) + B(t)K)x(t). \tag{10}$$

It is obvious that

$$\begin{aligned} \dot{x}(t-T) &= M(t-T, 2kT)x(2kT), \\ & t \in [2kT+T, 2kT+2T). \end{aligned} \tag{11}$$

Therefore, substituting Eq. (11) into Eq. (9), it can be obtained

$$\begin{aligned} \dot{x}(t) &= (A(t) + B(t)K)x(t) \\ &\quad - B(t)KM(t-T, 2kT)x(2kT). \end{aligned} \tag{12}$$

By left multiplying matrices $\Gamma^{-1}(t, 2kT+T)$ on both sides of Eq. (12) and formulation derivation, it is obtained

$$\begin{aligned} x(t) &= \{\Gamma(t-2kT-T, 0)M(T,0) \\ &\quad - \int_{2KT+T}^{t} \Gamma(t,\bar{t})B(\bar{t})KM(\bar{t}-T, 2kT)d\bar{t}\Big\} \cdot x(2kT), \\ &\quad t \in [2kT+T, 2kT+2T),\ \bar{t} \in [2kT+T, t]. \end{aligned} \tag{13}$$

Setting $\hat{t} = \bar{t} - 2kT$ yields

$$\begin{aligned} &\int_{2KT+T}^{t} \Gamma(t,\bar{t})B(\bar{t})KM(\bar{t}-T, 2kT)d\bar{t} \\ &= \int_{T}^{t-2KT} \Gamma(t, \hat{t}+2kT)B(\hat{t}+2kT)KM(\hat{t} \\ &\quad + 2kT - T, 2kT)d\hat{t}, \\ &\quad t \in [2kT+T, 2kT+2T). \end{aligned} \tag{14}$$

Since $\Gamma(t, \hat{t}+2kT) = \Gamma(t-2KT, \hat{t}), M(\hat{t}+2kT-T, 2kT) = M(\hat{t}-T, 0)$ and $B(\hat{t}+2kT) = B(\hat{t})$, it is obtained from Eq. (14)

$$\begin{aligned} &\int_{2KT+T}^{t} \Gamma(t,\bar{t})B(\bar{t})KM(\bar{t}-T, 2kT)d\bar{t} \\ &= \int_{T}^{t-2KT} \Gamma(t-2kT, \hat{t})B(\hat{t})KM(\hat{t}-T, 0)d\hat{t}. \end{aligned} \tag{15}$$

Then, it follows from Eqs. (13) and (15) that

$$x(t) = \Psi(t) \cdot x(2kT),\ t \in [2kT+T, 2kT+2T), \tag{16}$$

where

$$\Psi(t) = \Gamma(t-2kT-T,0)M(T,0) - \int_T^{t-2kT} \Gamma(t-2kT,\hat{t})B(\hat{t})KM(\hat{t}-T,0)d\hat{t}. \tag{17}$$

By setting $t = 2kT + 2T$, Eq. (17) becomes

$$\Psi(2T) = \Gamma(T,0)M(T,0) - \int_T^{2T} \Gamma(2T,\hat{t})B(\hat{t})KM(\hat{t}-T,0)d\hat{t}. \tag{18}$$

Equation (18) constructs a monodromy matrix for the closed-loop system (7) with the doubled period $2T$ such that

$$x(2kT+2T) = \Psi(2T)\cdot x(2kT),\ k = 0,1,2,\ldots. \tag{19}$$

Therefore, the stability of the closed-loop system is considered to be decided by the eigenvalues of the matrix $\Psi(2T)$.

3.2 The high-precision direct integration method

Let initial state of system (8) be $x(t_0) = x_0$. If we define a sequence of vectors $x_i(t) \in \Re^n (i = [0,\infty))$ on the closed interval $[t_0, t]$ as

$$\begin{cases} x_0(t) = x_0, \\ x_1(t) = x_0 + \int_{t_0}^t A(s_1)x_0(s_1)\mathrm{d}s_1, \\ x_2(t) = x_0 + \int_{t_0}^t A(s_1)x_1(s_1)\mathrm{d}s_1, \\ \vdots \\ x_i(t) = x_0 + \int_{t_0}^t A(s_1)x_{i-1}(s_1)\mathrm{d}s_1, \end{cases} \tag{20}$$

then, $x_i(t)$ can be rewritten as a sum of terms involving integrals of the matrix $A(t)$.

$$\begin{aligned} x_i(t) = x_0 &+ \int_{t_0}^t A(s_1)x_0\mathrm{d}s_1 \\ &+ \int_{t_0}^t A(s_1)\int_{t_0}^{s_1} A(s_2)x_0\mathrm{d}s_2\mathrm{d}s_1 + \ldots \\ &+ \int_{t_0}^t A(s_1)\int_{t_0}^t A(s_2)\cdots\int_{t_0}^{s_{i-1}} A(s_i)x_0\mathrm{d}s_i\cdots\mathrm{d}s_1. \end{aligned} \tag{21}$$

Assume the isometric division of time domain $[t_0, t_f]$ to be

$$t_{i+1} - t_i = \tau \equiv T/N \in [t_0, t_f],\ i = 0,1,2,\ldots. \tag{22}$$

Define $M(t,t_0)$ which is a function of two variables to be the transition matrix of system (8). It is obvious that there exists

$$x(t_{i+1)} = M(t_{i+1},t_i)x(t_i). \tag{23}$$

The transition matrix $M(t,t_0)$ can be expressed in the generalized Peano–Baker series as [63]

$$\begin{aligned} M(t,t_0) = I &+ \int_{t_0}^t A(s_1)\mathrm{d}s_1 \\ &+ \int_{t_0}^t A(s_1)\int_{t_0}^{s_1} A(s_2)\mathrm{d}s_2\mathrm{d}s_1 + \ldots \\ &+ \int_{t_0}^t A(s_1)\int_{t_0}^t A(s_2)\cdots\int_{t_0}^{s_{i-1}} A(s_i)\mathrm{d}s_i\cdots\mathrm{d}s_1. \end{aligned} \tag{24}$$

Then, a high-precision direct integration algorithm, named as HPDI algorithm, for calculating the transition matrix $M(t_{k+1},t_k)$ is established as follows.

Step 1: Finely divide the interval of $[t_k, t_{k+1}]$ into

$$t_k = t_0^k < t_1^k < t_2^k < \cdots < t_m^k = t_{k+1},$$

where $m = 2^Q$. Here, Q is a fine parameter, $t_{j+1}^k - t_j^k = \tau/m, j = 0,1,\ldots,m-1$.

Step 2: Compute, respectively, $A(t_j^k)$, $A((t_j^k + t_{j+1}^k)/2)$ and $A(t_{j+1}^k)$ based on Eq. (6). Here, the periodic solutions $\xi(t)$ are calculated numerically by fourth-order Runge–kutta method.

Step 3: From the properties of transfer matrix, it is obvious that

$$M(t_{k+1},t_k) = M(t_m^k, t_{m-1}^k)M(t_{m-1}^k, t_{m-2}^k)\cdots M(t_1^k, t_0^k).$$

Each transition matrix needs to be taken its third-order approximation of the following Peano–Baker series.

$$\begin{aligned} \tilde{M}(t_{j+1}^k, t_j^k) = I &+ [A(t_j^k) + 4A((t_j^k + t_{j+1}^k)/2) \\ &+ A(t_{j+1}^k)]d\tau/(3!) \\ &+ [2A(t_{j+1}^k)A(t_j^k) + A(t_j^k)A(t_{j+1}^k)](d\tau)^2/(3!) \\ &+ [A(t_j^k)]^3(d\tau)^3/(3!). \end{aligned} \tag{25}$$

If we define

$$\tilde{M}(t_{k+1},t_k) = \prod_{j=0}^{m-1} \tilde{M}(t_{j+1}^k, t_j^k), \tag{26}$$

then $\tilde{M}(t_{k+1},t_k)$ is the approximation of the transition matrix $M(t_{k+1},t_k)$.

Step 4: Calculate $\tilde{M}(t_{k+1},t_k)$.

$$\begin{aligned} \Lambda_j^0 \Leftarrow\ & [A(t_j^k) + 4A((t_j^k + t_{j+1}^k)/2) + A(t_{j+1}^k)]d\tau/(3!) \\ & + [2A(t_{j+1}^k)A(t_j^k) + A(t_j^k)A(t_{j+1}^k)](d\tau)^2/(3!) \\ & + [A(t_j^k)]^3(d\tau)^3/(3!),\ j = 0,1,2,\ldots,m-1; \end{aligned}$$

For $i = 1$ to Q

$$\Lambda_j^i = \Lambda_{2j+1}^{i-1} + \Lambda_{2j}^{i-1} + \Lambda_{2j+1}^{i-1}\Lambda_{2j}^{i-1},$$
$$j = 0, 1, 2, \ldots, 2^{Q-i} - 1;$$

End

$$\tilde{M}(t_{k+1}, t_k) \Leftarrow I + \Lambda_0^Q. \tag{27}$$

Step 5: Repeat executions of *Step* 2-4 for N times. Then, it can be obtained $\tilde{M}(t_1, t_0), \tilde{M}(t_2, t_1), \cdots, \tilde{M}(t_N, t_{N-1})$,, respectively.

Step 6: Calculate $M(t, t_0)$. If $t = T$, then

$$M(t, t_0) \simeq \tilde{M}(t_N, t_{N-1}) \cdots \tilde{M}(t_2, t_1)\tilde{M}(t_1, t_0), \tag{28}$$

else if $t < T$, then

$$M(t, t_0) \simeq \tilde{M}(t, t - \tau) \cdots \tilde{M}(t_2, t_1)\tilde{M}(t_1, t_0). \tag{29}$$

Based on the above HPDI algorithm, the transition matrices $M(T, 0)$ and $M(\hat{t} - T, 0)$ in Eq. (18) can be calculated by Eqs. (28) and (29), respectively.

In order to calculate the transition matrices $\Gamma(T, 0)$ and $\Gamma(2T, \hat{t})$ in Eq. (18), it is considered that $\hat{A}(t) = A(t) + B(t)K$. Then, similar to that of the transition matrices $M(T, 0)$ and $M(\hat{t} - T, 0)$, $\Gamma(T, 0)$ and $\Gamma(2T, \hat{t})$ can be calculated based on the same precise integration algorithm. Therefore, the monodromy matrix $\Psi(2T)$ in Eq. (18) which is associated with the closed-loop system (7) can be computed. By selecting an appropriate gain matrix K, the state trajectory of the system (7) converges toward a periodic solution.

4 Illustrative examples

In this section, we give two examples to examine the effectiveness of the above method.

4.1 Example 1

Consider a nonlinear system defined by a two-dimensional state vector $\mathbf{x} = [\mathbf{x}_1, \mathbf{x}_2]^T$, a control input vector $u = (u_1, u_2)$ and the vector field

$$\dot{\mathbf{x}} = f(\mathbf{x}, u)$$
$$\triangleq \begin{bmatrix} -\mathbf{x}_1\left(\mathbf{x}_1^2 + \mathbf{x}_2^2 - (\mathbf{x}_1^2 + \mathbf{x}_2^2)^2\right) + 2\pi\mathbf{x}_2 + u_1 \\ -\mathbf{x}_2\left(\mathbf{x}_1^2 + \mathbf{x}_2^2 - (\mathbf{x}_1^2 + \mathbf{x}_2^2)^2\right) - 2\pi\mathbf{x}_1 + u_2 \end{bmatrix}. \tag{30}$$

The above system (30) is a modified version of the exemplified system of the so-called Poincaré–Andronov–Hopf bifurcation [61]. The linear variational equation associated with the closed-loop system under the act-and-wait controller (with $T = 1$s) is given by Eq. (5), where

$$A(t) = \begin{bmatrix} 2\cos^2(2\pi t) & -\sin(4\pi t) + 2\pi \\ -\sin(4\pi t) - 2\pi & 2\sin^2(2\pi t) \end{bmatrix}, \tag{31}$$

$$B(t) = \begin{bmatrix} 1 & 0 \\ 0 & 1 \end{bmatrix}. \tag{32}$$

The system (30) shows unstable behavior if there is no control input. To evaluate the asymptotic behavior of solutions under the control law (2), it needs to examine the eigenvalues of the monodromy matrix $\Psi(2T)$ associated with the closed-loop system (7). Based on the proposed precise integration algorithm, by calculating numerically the value of $\Psi(2T)$ for a certain range of feedback gain parameters and search for an appropriate feedback gain matrix $K \in \mathfrak{R}^{2\times 2}$.

Note that for the feedback gain matrix $K = [2.2, 4.0; 4.5, -3.2]$, the corresponding monodromy matrix is calculated from Eq. (18) based on the HPDI algorithm discussed in Sect. 3.2 as

$$\Psi(2T) = \begin{bmatrix} 0.7052 & 0.0493 \\ 3.5138 & 0.3244 \end{bmatrix}. \tag{33}$$

which has the eigenvalues $\lambda_1 = 0.9726$ and $\lambda_2 = 0.057$.

Figure 2 plots a phase portrait of $(\mathbf{x}_1, \mathbf{x}_2)$ of the uncontrolled system (30) (with the control input $u = 0$) under the initial condition $\mathbf{x}_0 = (1, -0.1)$. From the time $t = 1.5$ s, the state trajectory begins to diverge from the periodic orbit. The periodic system without control input, hence, shows unstable behavior.

Figures 3 and 4, respectively, show a behavior and the phase portrait of the controlled system starting from the initial state $\mathbf{x}_0 = (1, -0.1)$. Figure 3 shows a behavior of the controlled system, while Figure 4 plots a phase portrait of $(\mathbf{x}_1, \mathbf{x}_2)$. It is known from Figs. 3 and 4 that the state trajectory converges to the periodic orbit, i.e.,

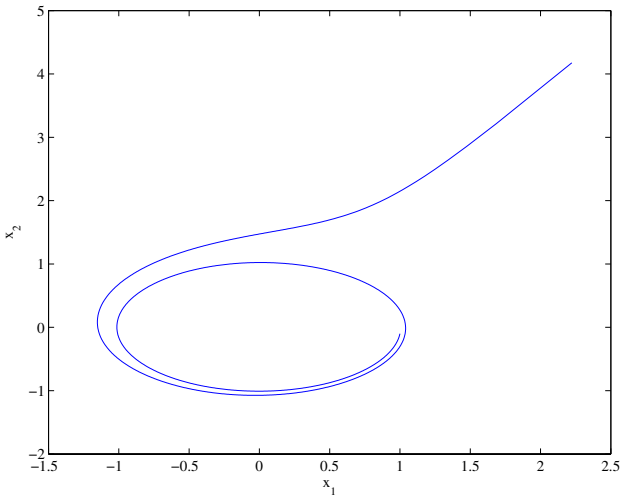

Fig. 2 The phase portrait of $\mathbf{x}_1 - \mathbf{x}_2$ of the system (30) without control input corresponding to the time of $t = [0, 1.8]$

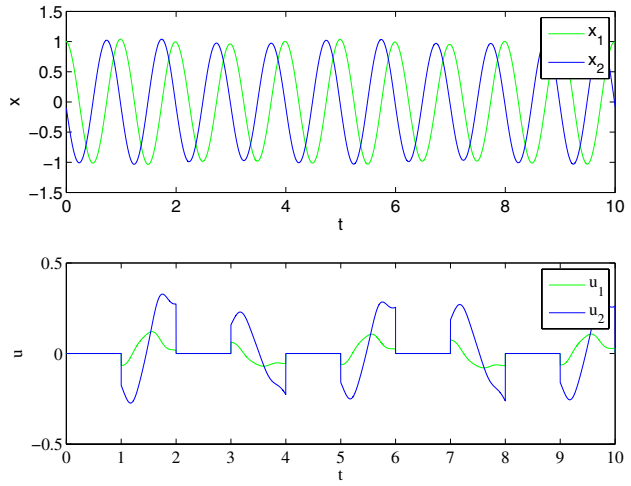

Fig. 3 The time history of $\mathbf{x}$ and u of the system (30) stabilized by act-and-wait DFC

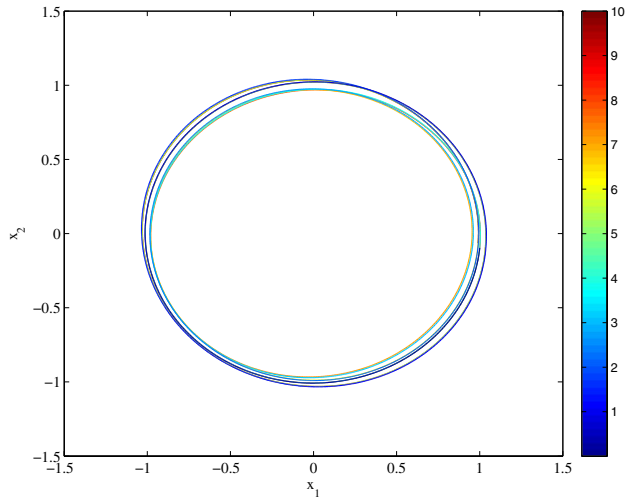

Fig. 4 The phase portrait of $\mathbf{x}_1 - \mathbf{x}_2$ of the system (30) stabilized by act-and-wait delayed feedback control; it is a colored 3D contour of time mapped on the bottom plain in which color-bar represents the time t (s)

system (30) reaches a stabilization state via the proposed method.

4.2 Example 2

As the next example, it is considered the well-known Lorenz system. The system is defined by a three-dimensional state vector $\mathbf{x} = [\mathbf{x}_1, \mathbf{x}_2, \mathbf{x}_3]^T$, a control input vector $u = (u_1, u_2)$ and the vector field

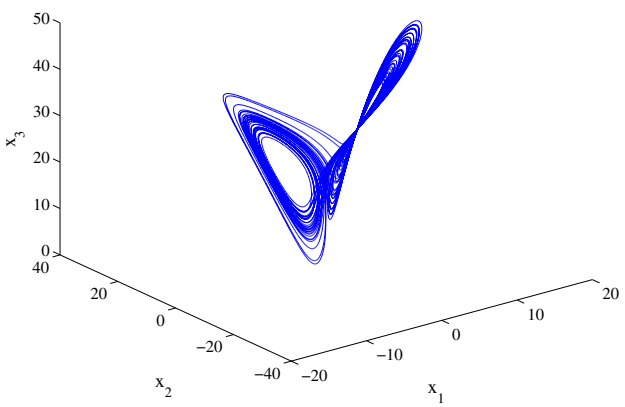

Fig. 5 The phase portrait of $\mathbf{x}_1 - \mathbf{x}_2 - \mathbf{x}_3$ of the system (34) without control input corresponding to the time of $t = [0, 50s]$

$$\dot{\mathbf{x}} = f(\mathbf{x}, u) \triangleq \begin{bmatrix} -\sigma(\mathbf{x}_1 - \mathbf{x}_2) \\ \gamma\mathbf{x}_1 - \mathbf{x}_2 - \mathbf{x}_1\mathbf{x}_3 + u \\ \mathbf{x}_1\mathbf{x}_2 - b\mathbf{x}_3 \end{bmatrix}, \tag{34}$$

where $\sigma = 10, \gamma = 28$ and $b = 8/3$.

If choosing the period-one UPO with the period $T = 1.5586\,s$ and the initial conditions $\mathbf{x}_0 = [-15.467, -15.411, 36.598]$, the linear variational equation associated with the closed-loop system under the act-and-wait controller is given by Eq. (5), where

$$A(t) = \begin{bmatrix} -\sigma & \sigma & 0 \\ \gamma - \mathbf{x}_3 & -1 & -\mathbf{x}_1 \\ \mathbf{x}_2 & \mathbf{x}_1 & -b \end{bmatrix}, \qquad B(t) = \begin{bmatrix} 0 & 1 & 0 \end{bmatrix}^T. \tag{35}$$

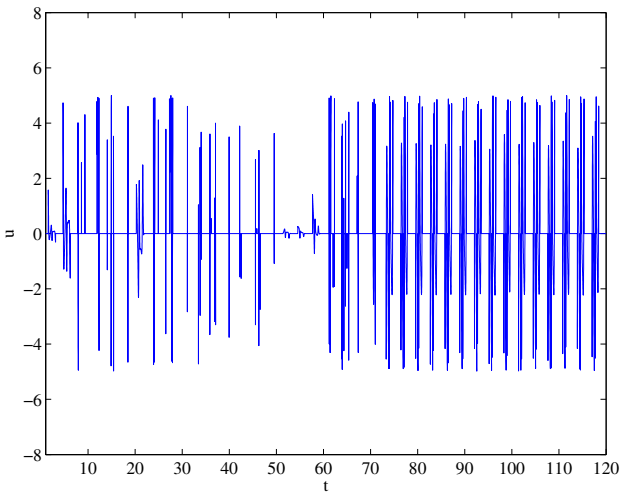

Fig. 6 The stabilization control input of the system (34) stabilized by act-and-wait delayed feedback control

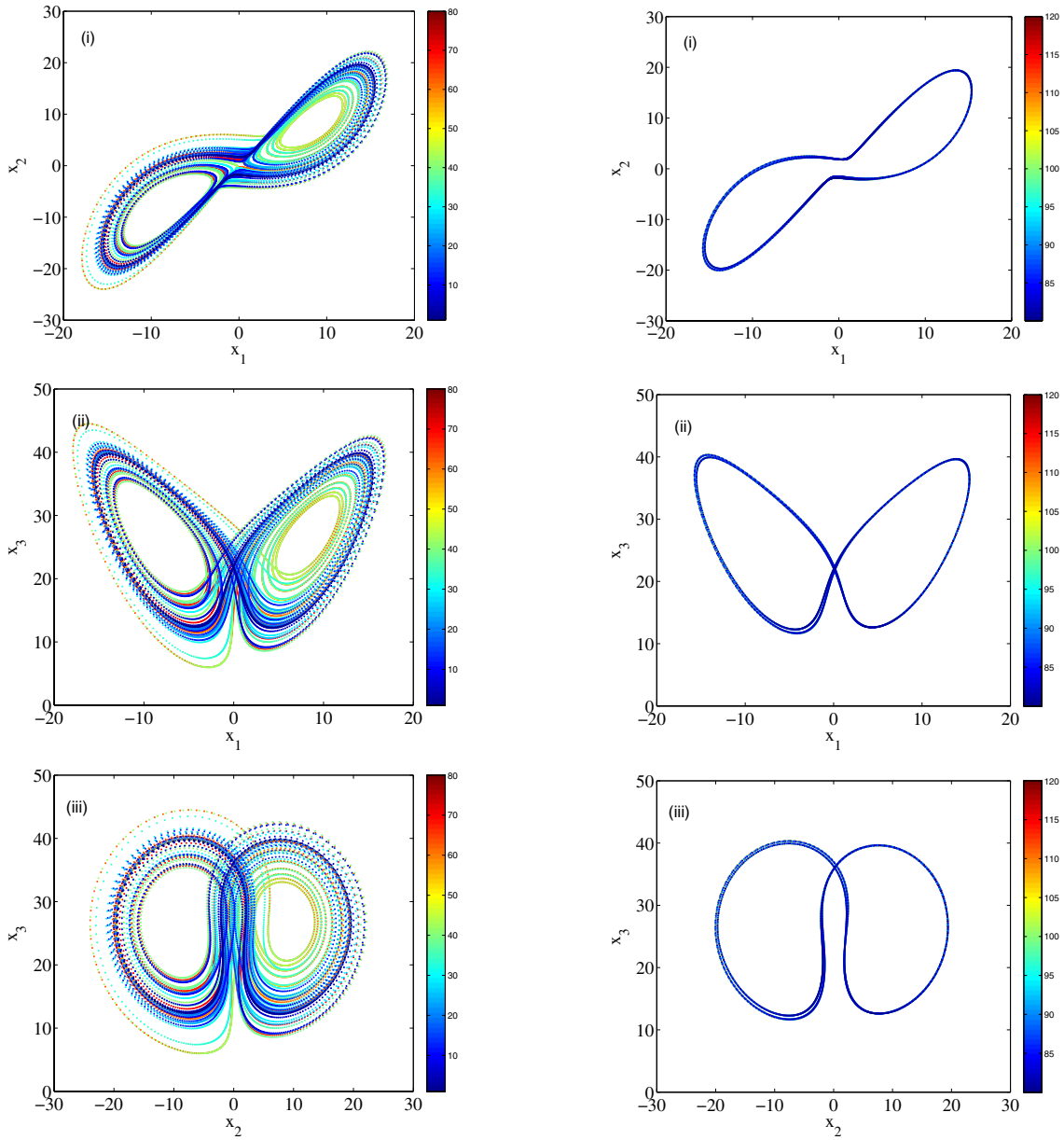

(a) Phase portrait (t=0∼80[s]) **(b)** Phase portrait (t=80∼120[s])

Fig. 7 The phase portrait of $\mathbf{x}_i - \mathbf{x}_j (i = 1, 2; j = 2, 3)$ of the system (34) stabilized by act-and-wait delayed feedback control; it is a colored 3D contour of time mapped on the bottom plain in which color-bar represents the time t (s)

The monodromy matrix associated with the uncontrolled system is given by

$$M(T,0) = \begin{bmatrix} 1.2257 & 1.3786 & -1.4541 \\ 7.3979 & 9.9107 & -9.4232 \\ 4.0485 & 6.0767 & -5.4226 \end{bmatrix}, \tag{36}$$

which has the eigenvalues 4.7148, 0, and 0.9991. As shown in Fig. 5, the uncontrolled system (34) shows chaotic behavior.

Then, performing the procedures similar to those described in the previous example, it can be achieved the successful control of the UPO.

For the feedback gain matrix $K = [-4.1, -5.0, -3.8]$, the corresponding monodromy matrix $\Psi(2T)$ is calculated from Eq.(18) as

$$\Psi(2T) = \begin{bmatrix} 0.0080 & 0.0543 & -0.0281 \\ 1.1896 & 3.4808 & -2.2845 \\ 1.6234 & 4.5691 & -3.0435 \end{bmatrix}, \tag{37}$$

which has the eigenvalues $\lambda_1 = 0.6927, \lambda_2 = -0.0001$and $\lambda_3 = -0.2473$.

Figure 6 plots the time history of the control input of the system (34) stabilized by the proposed method. The trajectory of the orbits in the phase plane $\mathbf{x}_i - \mathbf{x}_j (i = 1, 2; j = 2, 3)$ from t=0 till t=120 s via the stabilization control input u is shown in Fig. 7. The initial condition $\mathbf{x}_0 = (-15.46, -15.41, 36.59)$. The phase portraits of $\mathbf{x}_1 - \mathbf{x}_2, \mathbf{x}_1 - \mathbf{x}_3, \mathbf{x}_2 - \mathbf{x}_3$ are shown in (i), (ii), (iii), respectively. Fig. 7a depicts the trajectory of $0 \sim 80$ s and Fig. 7b plots that of $80 \sim 120$ s. From Fig. 7b and Fig. 6, it is obvious that the trajectory of the orbits from about 70 s converged closer to a closed curve which means that the system attained a stable orbit via the act-and-wait delayed feedback control.

5 Conclusion

This paper developed a stabilization method for the periodic orbits embedded in nonlinear chaotic systems via an act-and-wait delayed feedback control. The proposed method derived a finite-sized corresponding monodromy matrix for the closed-loop system under a switching mechanism that turns the delayed feedback controller on and off alternately at every integer multiples of the period of the desired UPO. By analyzing the eigenvalues of the corresponding monodromy matrix, it was obtained conditions under which the state trajectory converges toward a periodic solution. Due to the fact that it is hard to find a homogeneous expression of the monodromy matrix corresponding to the act-and-wait DFC, we present a periodically time-varying precise integration method by which the transition matrices can be calculated numerically with a high precision. Furthermore, two numerical examples showed that the dynamics of nonlinear systems can be stabilized to periodic orbits by means of the proposed strategy.

Acknowledgements The authors thank the anonymous reviewers and the editor-in-chief for their valuable suggestions that helped improve the quality of this manuscript.

Funding This study was funded by a Grant from the national key research and development program of China (Grant No. 2018YFC0807405).

Compliance with ethical standards

Conflict of interest The authors declare that they have no conflict of interest.

References

1. Ghayesh MH, Farokhi H (2015) Chaotic motion of a parametrically excited microbeam. Int J Eng Sci 96:34–45
2. Ghayesh MH, Farokhi H, Farajpour A (2018) Chaotic oscillations of viscoelastic microtubes conveying pulsatile fluid. Microfluid Nanofluid 22(7):72. https://doi.org/10.1007/s10404-018-2091-z
3. Ghayesh MH, Farokhi H (2017) Global dynamics of imperfect axially forced microbeams. Int J Eng Sci 115:102–116. https://doi.org/10.1016/j.ijengsci.2017.01.005
4. Farokhi H, Ghayesh MH, Hussain S (2015) Three-dimensional nonlinear global dynamics of axially moving viscoelastic beams. J Vib Acoust 138(1):1. https://doi.org/10.1115/1.4031600,011007
5. Ghayesh MH, Amabili M (2013) Non-linear global dynamics of an axially moving plate. Int J Non-Linear Mech 57:16–30. https://doi.org/10.1016/j.ijnonlinmec.2013.06.005
6. Ghayesh MH, Amabili M, Farokhi H (2013) Two-dimensional nonlinear dynamics of an axially moving viscoelastic beam with time-dependent axial speed. Chaos Solitons Fract 52:8–29. https://doi.org/10.1016/j.chaos.2013.03.005
7. Ghayesh MH, Amabili M (2013) Post-buckling bifurcations and stability of high-speed axially moving beams. Int J Mech Sci 68:76–91. https://doi.org/10.1016/j.ijmecsci.2013.01.001
8. Liu D, Yamaura H (2012) Chaos control of a phi6 -van der pol oscillator driven by external excitation. Nonlinear Dyn 68(1–2):95–105
9. Ghayesh MH, Amabili M, Païdoussis MP (2012) Nonlinear vibrations and stability of an axially moving beam with an intermediate spring support: two-dimensional analysis. Nonlinear Dyn 70(1):335–354. https://doi.org/10.1007/s11071-012-0458-3
10. Ghayesh MH (2012) Stability and bifurcations of an axially moving beam with an intermediate spring support. Nonlinear Dyn 69(1):193–210. https://doi.org/10.1007/s11071-011-0257-2
11. Ott E, Grebogi C, Yorke J (1990) Controlling chaos. Phys Rev Lett 64(11):1196–1199
12. Pyragas K (1992) Continuous control of chaos by self-controlling feedback. Phys Lett A 170(6):421–428. https://doi.org/10.1016/0375-9601(92)90745-8
13. Zoldi SM, Franceschini G, Bose S, Schöll E (2000) Stabilizing unstable periodic orbits in reaction-diffusion systems by global time-delayed feedback control
14. Postlethwaite CM, Silber M (2007) Stabilizing unstable periodic orbits in the lorenz equations using time-delayed feedback control. Phys Rev E Stat Nonlinear Soft Matter Phys 76(5 Pt 2):056214
15. Botmart T, Niamsup P, Liu X (2010) Synchronization of nonautonomous chaotic systems with time-varying delay via delayed feedback control. Commun Nonlinear Sci Numer Simul 17(4):1894–1907
16. Fang Y, Shi Z (2015) Chaos analysis and delayed-feedback control in a discrete dynamic coupled map traffic model. Physica A 422:40–46. https://doi.org/10.1016/j.physa.2014.11.038
17. Redhu P, Gupta AK (2015) Delayed-feedback control in a lattice hydrodynamic model. Commun Nonlinear Sci Numer Simul 27(1–3):263–270
18. Leonov GA, Moskvin AV (2017) Stabilizing unstable periodic orbits of dynamical systems using delayed feedback control with periodic gain. Int J Dyn Control 6(12):1–8
19. Nategh M, Baleanu D, Taghizadeh E, Gilani ZG (2017) Almost local stability in discrete delayed chaotic systems. Nonlinear Dyn 89(4):1–10
20. Ushio T, Yamamoto S (1999) Prediction-based control of chaos. Phys Lett A 264(1):30–35. https://doi.org/10.1016/S0375-9601(99)00782-3

21. Hino T, YAMAMOTO S, USHIO T (2002) Stabilization of unstable periodic orbits of chaotic discrete-time systems using prediction-based feedback control. Int J Bifurc Chaos 12(02):439–446
22. Soukkou A, Boukabou A, Leulmi S (2016) Prediction-based feedback control and synchronization algorithm of fractional-order chaotic systems. Nonlinear Dyn 85(4):1–24
23. Fuh CC, Tung PC (1996) Robust control for a class of nonlinear oscillators with chaotic attractors. Phys Lett A 218(3–6):240–248. https://doi.org/10.1016/0375-9601(96)00395-7
24. Cleju M (2014) About robust control on nonlinear chaotic oscillators. In: International conference and exposition on electrical and power engineering
25. Nazzal JM, Natsheh AN (2007) Chaos control using sliding-mode theory. Chaos Solitons Fract 33(2):695–702. https://doi.org/10.1016/j.chaos.2006.01.071
26. Salarieh H, Alasty A (2009) Control of stochastic chaos using sliding mode method. J Comput Appl Math 225(1):135–145. https://doi.org/10.1016/j.cam.2008.07.032
27. Park J, Lee J, Won S (2015) Adaptive sliding mode control for stabilization of stochastic chaotic systems with multi-constraints. In: Control conference
28. Gui-Yuan FU, Zhong-Shen LI (2010) Adaptive control for a class of chaotic systems with unknown parameters. In: Chinese control and decision conference
29. Wang X, Wang Y (2011) Adaptive control for synchronization of a four-dimensional chaotic system via a single variable. Nonlinear Dyn 65(3):311–316
30. Luo Runzi (2015) The robust adaptive control of chaotic systems with unknown parameters and external disturbance via a scalar input. Int J Adapt Control Signal Process 29(10):1296–1307
31. Ahrabi AR, Kobravi HR (2019) A chaos to chaos control approach for controlling the chaotic dynamical systems using hamilton energy feedback and fuzzy-logic system. Chaos: Interdiscipl J Nonlinear Sci 29(7):073113
32. Ushio T (1996) Limitation of delayed feedback control in nonlinear discrete-time systems. IEEE Trans Circuits Syst I Fundam Theory Appl 43(9):815–816. https://doi.org/10.1109/81.536757
33. Just W, Bernard T, Ostheimer M, Reibold E, Benner H (1997) Mechanism of time-delayed feedback control. Phys Rev Lett 78(2):203–206. https://doi.org/10.1103/PhysRevLett.78.203
34. Pyragas K (1995) Control of chaos via extended delay feedback. Phys Lett A 206(5–6):323–330. https://doi.org/10.1016/0375-9601(95)00654-L
35. Woo-Sik WS, Young-Jai YJ, Jung-Wan JW, Dong-Uk DU, Chil-Min CM (2006) Control of a deterministic inertia ratchet system via extended delay feedback. J- Kor Phys Soc 50(91):243–248
36. Guo Y, Jiang W, Niu B (2013) Bifurcation analysis in the control of chaos by extended delay feedback. J Frankl Inst 350(1):155–170
37. Liu D, Yan G, Yamaura H (2014) Dynamic delayed feedback control for stabilizing the giant swing motions of an underactuated three-link gymnastic robot. Nonlinear Dyn 78(1):147–161
38. Rong Y, Wen H (2018) An extended delayed feedback control method for the two-lane traffic flow. Nonlinear Dyn 94:1–12
39. Yamamoto S, Ushio T (2002) Stabilization of chaotic discrete-time systems by periodic delayed feedback control. In: Proceedings of the American control conference, vol 3, pp 2260–2261
40. Just W, Popovich S, Amann A, Baba N, Schöll E (2003) Improvement of time-delayed feedback control by periodic modulation: analytical theory of floquet mode control scheme. Phys Rev E 67(2):026222. https://doi.org/10.1103/PhysRevE.67.026222
41. Liu D, Yan G (2013) Stabilization of discrete-time chaotic systems via improved periodic delayed feedback control based on polynomial matrix right coprime factorization. Nonlinear Dyn 74(4):1243–1252
42. Leonov GA, Zvyagintseva KA, Kuznetsova OA (2016) Pyragas stabilization of discrete systems via delayed feedback with periodic control gain. IFAC-PapersOnLine 49(14):56–61. https://doi.org/10.1016/j.ifacol.2016.07.979
43. Lu J, Ma Z, Li L (2009) Double delayed feedback control for the stabilization of unstable steady states in chaotic systems. Commun Nonlinear Sci Numer Simul 14(7):3037–3045
44. Wu N, Ying H (2017) Stabilization of wave segments under a delayed feedback in the parameter space. Nonlinear Dyn 89(4):2603–2608
45. Costa DDA, Savi MA (2018) Chaos control of an sma-pendulum system using thermal actuation with extended time-delayed feedback approach. Nonlinear Dyn 93(2):571–583
46. Paul B, Banerjee T (2019) Nonlocal time-delayed feedback control of spatiotemporal patterns: controlling a network of digital phase-locked loops. Nonlinear Dyn 96:1–13
47. Stépán G, Insperger T (2006) Stability of time-periodic and delayed systems—a route to act-and-wait control. Ann Rev Control 30(2):159–168. https://doi.org/10.1016/j.arcontrol.2006.08.002
48. Insperger T (2006) Act-and-wait concept for continuous-time control systems with feedback delay. IEEE Trans Control Syst Technol 14(5):974–977. https://doi.org/10.1109/TCST.2006.876938
49. Insperger T, Kovacs LL, Galambos P, Stepan G (2010) Increasing the accuracy of digital force control process using the act-and-wait concept. IEEE/ASME Trans Mechatron 15(2):291–298. https://doi.org/10.1109/TMECH.2009.2024683
50. Insperger T, Stepan G (2015) Act-and-wait control concept for discrete-time systems with feedback delay. Iet Control Theory Appl 1(3):553–557
51. Pyragas V, Pyragas K (2018) Act-and-wait time-delayed feedback control of autonomous systems. Phys Lett A 382(8):574–580. https://doi.org/10.1016/j.physleta.2017.12.019
52. Pyragas V, Pyragas K (2016) Act-and-wait time-delayed feedback control of nonautonomous systems. Phys Rev E 94(1–1):012201. https://doi.org/10.1103/PhysRevE.94.012201
53. Bin Mohd Taib MAF, Hayakawa T, Cetinkaya A (2013) Delayed feedback control for linear time-varying periodic systems in act-and-wait fashion. IFAC Proc Vol 46(12):11–16. https://doi.org/10.3182/20130703-3-FR-4039.00041
54. Cetinkaya A, Hayakawa T, Mohd Taib MAFB (2018) Stabilizing unstable periodic orbits with delayed feedback control in act-and-wait fashion. Syst Control Lett 113:71–77. https://doi.org/10.1016/j.sysconle.2018.01.010
55. Insperger T, Stepan G (2010) On the dimension reduction of systems with feedback delay by act-and-wait control. IMA J Math Control Inf 27(4):457–473
56. Konishi K, Kokame H, Hara N (2011) Delayed feedback control based on the act-and-wait concept. Nonlinear Dyn 63(3):513–519. https://doi.org/10.1007/s11071-010-9819-y
57. Pyragiene T, Pyragas K (2015) Anticipating chaotic synchronization via act-and-wait coupling. Nonlinear Dyn 79(3):1901–1910
58. Wang J, Kuske R (2017) The influence of parametric and external noise in act-and-wait control with delayed feedback. Chaos Interdiscipl J Nonlinear Sci 27(11):114319

59. Zhou G, Jiang L (2005) A high precision direct integration method for periodically time-varying linear system. J Shanghai Jiaotong Univ 39(6):1016–1019
60. Li K, Darby AP (2009) A high precision direct integration scheme for nonlinear dynamic systems. J Comput Nonlinear Dyn 4(4):1724–1732
61. Khalil H (2002) Nonlinear systems. Prentice Hall, New Jersey
62. Gjurchinovski A, Urumov V (2013) Stabilization of unstable steady states and unstable periodic orbits by feedback with variable delay. Roman. Rep. Phys. 58:36–49
63. Dacunha JJ (2005) Transition matrix and generalized matrix exponential via the peano-baker series. J Differ Equ Appl 11(15):20